Research Article Vol. 33, No. 16 / 11 Aug 2025 / Optics Express 33077
Optics EXPRESS

Forward transmission distributed sensing with variational mode decomposition for near-identical frequency vibration monitoring

HANJIE LIU,[1,2,3] XING RAO,[1,2,3] SHANGWEI DAI,[1,2,3] GUOQIANG LIU,[1,2,3] RUNLONG ZHU,[1,2,3] GEORGE Y. CHEN,[1,2,3,*] AND YIPING WANG[1,2,3]

[1]*The Shenzhen Key Laboratory of Photonic Devices and Sensing Systems for Internet of Things, China*
[2]*Guangdong and Hong Kong Joint Research Centre for Optical Fibre Sensors, State Key Laboratory of Radio Frequency Heterogeneous Integration, China*
[3]*Shenzhen Key Laboratory of Ultrafast Laser Micro/Nano Manufacturing, Key Laboratory of Optoelectronic Devices and Systems of Ministry of Education/Guangdong Province, College of Physics and Optoelectronic Engineering, Shenzhen University, Shenzhen 518060, China*
[*]*gychen@szu.edu.cn*

Abstract: Forward transmission-based distributed fiber-optic sensing is known for its long sensing distance, high signal-to-noise ratio and ease of integration with fiber-optic communication systems. It facilitates a straightforward approach for detecting sounds/vibrations and their positions. However, due to the cumulative nature of light propagation, this type of sensing technology is bottlenecked by iits inability to identify and position vibrations that share the same frequency. Fortunately, spatially separated vibration sources are unlikely to generate the exact frequency, due to non-identical material/structure characteristics. Even the same perturbation source can lead to different wavefronts of slightly different frequencies, due to minor variations in local density. To address the identical-frequency problem, we propose a solution combining variational mode decomposition (VMD) with the cross-correlation algorithm to analyze and spatially separate near-frequency vibration signals with a resolution of 0.005 Hz. The experimental results demonstrate the single-point vibration positioning ability of the proposed algorithm within the 4-10 Hz frequency range. At a vibration frequency of 10 Hz, positioning accuracies of 411.5 m (RMSE) and 405.2 m (standard deviation) were achieved. Concurrently, the methodology validated at 10 Hz exhibits effective multi-point positioning ability with precise signal frequency separation (0.01 Hz). The effectiveness of the method was further validated in processing broadband signals over a 40 km sensing fiber.

1. Introduction

Forward transmission based distributed sensing (FTDS) is an emerging sensing technology for detecting and positioning vibration/acoustic signals, which has been proved to be suitable for both terrestrial and marine environments due to its long sensing distance (100 km scale) and ease of integration with fiber-optic communication systems [1–3]. In natural phenomena such as earthquakes and tsunamis, as well as human activities such as construction zones and shipping lanes, can produce vibration signals of near-identical frequency at different locations. A sensor could also detect wavefronts of slightly different frequencies from a single perturbation source, due to minor variations in local material density. Therefore, distinguishing perfectly identical signal frequencies is not necessary, and co-frequency separation is sufficient for a large number of scenarios.

The dominant vibration positioning method for FTDS involves the cross-correlation (CC) of time-domain signals [4]. A significant limitation of this approach is that, while cross-correlation

#561898 https://doi.org/10.1364/OE.561898
Journal © 2025 Received 11 Mar 2025; revised 30 Jun 2025; accepted 3 Jul 2025; published 29 Jul 2025

Optics EXPRESS

is suitable for analyzing the delay between two highly correlated signals presenting a single vibration position (either single frequency or broadband), in practice the signals received at the two detection ends are slightly different due to noise and varying states of polarization, and thus the algorithm can no longer accurately determine the delay [5]. To address this problem, Wang et al [6] proposed a time shifting deviation (TSDEV) method to improve the position accuracy. However, this method is computation intensive, and it is still limited to single-point vibration event positioning (e.g. single frequency). The recently reported phase-spectrum time delay method employs Fourier transform techniques, where vibration amplitude and frequency information is obtained from the Fourier amplitude spectrum, while vibration position information associated with different signal frequencies is derived from the difference in the Fourier phase spectra [7]. This approach is relatively straightforward and proves advantageous for resolving multiple simultaneous vibration events. However, according to the current reports in the literature, this method can distinguish multi-point vibration events with a minimum frequency difference of approximately 20 Hz [8]. Additionally, this method is susceptible to background noise, which can affect phase calculations, thereby affecting the positioning accuracy.

Variational mode decomposition (VMD) is non-recursive and adaptive signal processing method, which can decompose the original signal into various frequency components and possesses the capability to filter out white noise [9]. Recently, it has demonstrated excellent results in the noise suppression of Sagnac fiber sensors [10], multiple-event recognition in distributed acoustic sensing (DAS) systems [11], negative pressure wave [12] etc.

To address the urgent need to separate near-identical frequency signals in FTDS, we adapt the powerful VMD algorithm for detecting approximately equal-frequency vibrations and resolving positions. The frequency resolution of the VMD algorithm can refined down to 0.005 Hz by appropriately selecting the sampling rate and the number of sampling points. The number of modal components within the VMD is determined through the application of permutation entropy (PE). The original signal obtained from the optical fiber sensor is decomposed into the corresponding number of intrinsic mode functions (IMF), where each component exhibits a limited bandwidth. Noise at zero frequency is filtered out, while retaining the IMFs that correspond to multi-point vibrations with 0.01 Hz separation. The time delay between the vibration signals is obtained through cross-correlation analysis of the decomposed IMFs, thereby enabling the positioning of multiple (even near-identical frequency) vibrations. In addition, both theoretical simulations and experimental verification are conducted to reveal the current level of performance with the available hardware. To the best of our knowledge, this is the first report of using VMD for identifying co-frequency signals in distributed sensing, which also solves a major bottleneck for FTDS technology.

2. Principle

2.1. System setup

The structure of the forward transmission distributed sensing system is shown in Fig. 1. It consists of the following modules: a narrow linewidth laser, two circulators (CIR), an isolator (ISO), a sensing fiber, two Mach-Zehnder interferometers (MZI) consisting of couplers and sensing fiber, four balance detectors (BD), two 90° optical hybrids and a four-channel oscilloscope (OSC). Upon traversing the ISO, continuous light is separated at 1×2 coupler1, resulting in two distinct beams denoted as I_1 and I_2, represented by green and red arrows, respectively. The beam I_1 undergoes further division into two additional beams, I_{12} and I_{11}, through 1×2 coupler2, while the beam I_2 is similarly split into I_{22} and I_{21}. An analysis of the optical pathway reveals that the signal light I_{22} interferes with the light-beam I_{11} at 2×2 coupler1, following their passage through two CIRs and sensing fiber. Similarly, the light-beam I_{21} also experiences interference with signal light I_{11} at 2×2 coupler2, adhering to the same underlying principles.

Optics EXPRESS

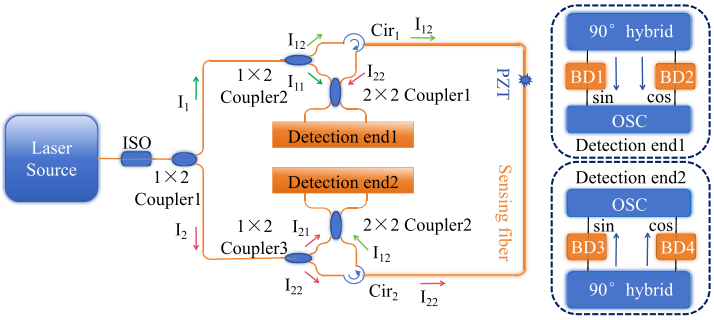

Fig. 1. FTDS system. ISO: Isolator; Cir: circulator; BD: balance detector; OSC: Oscilloscope.

The two interference signals of the 2×2 coupler1 output, after passing through the 90° hybrid and being detected by BD1 and BD2 under ideal conditions, can be expressed as:

$$I_k = A + B\cos(\varphi_1(t-t_1) - \frac{\pi}{2}(k-1)), k = 1, 2 \tag{1}$$

where A is the average optical power of the detected signals, B is the amplitude of the interference signal, and $\varphi_1(t-t_1) = \varphi_v(t-t_1) + \varphi_{noise}(t-t_1)$ is the phase shift caused by vibration event $\varphi_v(t-t_1)$ and noise $\varphi_{noise}(t-t_1)$. t_1 is the transit time for light to propagate from the vibration position to detection end 1.

The two interference signals of the 2×2 coupler2 output, after passing through the 90° optical hybrid and detected by BD1 and BD2 under ideal conditions, can be expressed as:

$$I_i = A + B\cos(\varphi_2(t-t_2) - \frac{\pi}{2}(i-1)), i = 1, 2 \tag{2}$$

where t_2 is the transit time for light to propagate from the vibration position to detection end 2.

The time-of-flight difference for light to propagate along the path of: vibration position→detection end 1 and vibration position→detection end 2 can obtained from time-domain cross-correlation and expressed as:

$$\Delta t = t_1 - t_2 \tag{3}$$

Thus, the middle position of the vibration acting on a segment of the sensing fiber from detection end 1 can be calculated through $c\Delta t/n$, where c is the velocity of light in vacuum, and n is the effective index of the fiber core. As the total fiber length of the sensing system L is already known, the vibration position can be determined from:

$$Z_m = \frac{1}{2}\left(L + \frac{c\Delta t}{n}\right) \tag{4}$$

It is worth noting that the aforementioned time-difference-based positioning approach is susceptible to noise and dispersion, which diminishes the accuracy of the positioning results. Furthermore, the cross-correlation algorithm is only suitable for resolving a single vibration source of fixed frequency. Although existing algorithms, such as phase-spectrum time delay, have demonstrated their capability to measure multi-point vibrations, they operate accurately only on vibration events with relatively large frequency differences, typically ranging from tens to hundreds of hertz. Consequently, vibration signal frequencies that are almost identical are indistinguishable from one another and treated as the same signal.

Optics EXPRESS

2.2. Near-identical frequency vibration positioning based on VMD

The Variational Mode Decomposition (VMD) algorithm is a non-recursive, adaptive method for signal processing. It is capable of decomposing a finite number of bandwidth-limited intrinsic mode functions (IMFs) along with their corresponding amplitude and phase from the original signal [13], which aids in the identification of approximate co-frequency vibration events and effectively suppressing the mode-alignment artifacts inherent to Empirical Mode Decomposition (EMD). In addition, it has been demonstrated that this method exhibits remarkable decomposition performance in environments dominate by white noise [14].

Taking the propagation of light along the path of detection end 1 as an example, a variational model of the original vibration-induced phase signal $\varphi(t)$ is established to minimize the sum of the bandwidths of all IMFs by using the 2-norm signal gradient, which can be expressed as [15]:

$$\begin{cases} \min\limits_{\{\varphi_n\},\{\omega_n\}} \left\{ \sum\limits_n \left\| \partial_t \left[\left(\delta(t) + \frac{j}{\pi t} \right) * \varphi_n(t) \right] e^{-j\omega_n t} \right\|_2^2 \right\} \\ \text{s. t.} \sum\limits_{n=1}^{N} \varphi_n = f(t) \end{cases} \tag{5}$$

where $\{\varphi_n\} = \{\varphi_1, \ldots, \varphi_n\}$ and $\{\omega_n\} = \{\omega_1, \ldots, \omega_n\}$ represent all IMF components of the original vibration signal and their corresponding center frequencies, respectively, N is the total number of IMF components, $\delta(t)$ is the unit impulse function, and "$*$" represents linear convolution.

By introducing the quadratic penalty factor and the Lagrangian operator, the aforementioned variational problem is reformulated into an unconstrained optimization problem that can be addressed using the alternative direction method of multipliers (ADMM) algorithm. The estimated IMFs and center frequency in the frequency domain can be expressed as:

$$\hat{\varphi}_n^{i+1}(\omega) = \frac{\hat{\varphi}(\omega) - \sum_{m \neq n} \hat{\varphi}_m(\omega) + \frac{\hat{\lambda}(\omega)}{2}}{1 + 2(\omega - \omega_n)^2} \tag{6}$$

$$\omega_n^{i+1} = \frac{\int_0^\infty \omega |\hat{\varphi}_n(\omega)|^2 \mathrm{d}\omega}{\int_0^\infty |\hat{\varphi}_n(\omega)|^2 \mathrm{d}\omega} \tag{7}$$

where "$\hat{}$" means take a Fourier transform, λ is the Lagrangian operator.

Based on Eq. (6), it can be observed that the obtained Intrinsic Mode Functions (IMFs) correspond to the output of the Wiener filter. In order to avoid the phenomenon of frequency aliasing, it is very important to accurately select the number of IMF components. The permutation entropy (PE) offers enhanced noise resilience due to its inherent insensitivity to Gaussian white noise, making it suitable for high-noise environments. It also offers superior computational efficiency featuring lower time complexity than approximate entropy or sample entropy, which promotes real-time signal processing. Therefore, PE method is chosen as a metric for evaluating the number of decomposed IMFs.

For a given time series $\{g(i), i = 1, 2, \cdots, N\}$, the corresponding phase space reconstruction matrix can be formulated as:

$$V = \begin{bmatrix} g(1) & g(1+t) & \cdots & g(1+(m-1)t) \\ g(2) & g(2+t) & \cdots & g(2+(m-1)t) \\ g(n) & g(n+t) & \cdots & g(n+(m-1)t) \\ \vdots & \vdots & \cdots & \vdots \\ g(y) & g(y+t) & \cdots & g(y+(m-1)t) \end{bmatrix} \tag{8}$$

Optics EXPRESS

where $y = N - (m-1)t$ denotes the number of reconstructive components, τ represents the time lag (commonly set to 1), and m corresponds to the embedding dimension (typically in the range 3–6).

To establish an ordered representation of the reconstructed components, we apply a permutation procedure based on ascending magnitude:

$$g(i+(n_1-1)t) \le g(i+(n_2-1)t) \le \cdots \le g(i+(n_m-1)t) \tag{9}$$

where $g(i+(n_1-1)t) \le g(i+(n_2-1)t)$ is the permutation index vector satisfying $n_1 < n_2$. This ordering mechanism ensures that component sequences are systematically arranged according to their numerical values.

For any arbitrary component row in the reconstructed matrix, a sequence of symbolic representations can be generated through dimension-wise mapping:

$$S(l) = \{n_1, n_1, \ldots, n_m\} \tag{10}$$

Where $l \in \{1,2,\ldots,h\}$ and $h \le m!$, implying that $m!$ distinct permutation groups can be formed under m-dimensional phase space mapping.

Let P_h denote the occurrence probability of each unique symbol sequence. Following Shannon's entropy principles, the permutation entropy (PE) of h-order temporal sequences for a given time series $g(i)$ is mathematically defined as:

$$PE = -\sum_{l=1}^{h} P_l \mathrm{In} P_l \tag{11}$$

This entropy metric quantifies the complexity of time series behavior, where a higher entropy value indicates a more complex and random decomposition signal, while a lower entropy value reflects a simpler and more regular decomposition signal [16]. Consequently, the number of IMFs within the VMD algorithm was optimized by the minimum average entropy.

The proposed method was employed to analyze the original vibration signals from the two-terminal forward transmission based distributed sensing system. This process involves the decomposition of the signals to eliminate the zero-frequency noise component while preserving the remaining IMFs of the vibration-induced phase signals. Subsequently, the time difference between the IMFs from detection end 1 and 2 is determined using a cross-correlation algorithm, thereby allow the position of the vibration-affected fiber segment to be estimated.

2.3. Simulation

The near co-frequency vibration signals are denoted by phi_i = $a_i + b_i$, $a_i = \sin(2*\pi*f_1*(t+ti))$, $b_i = \sin(2*\pi*f_2*(t+T_i))$, where $f_1 = 10$ Hz, $f_2 = 10.1$ Hz, $t_1 = 0$, $t_2 = 1/(2*f_1)$, $T_1 = 1/(2*f_2)$, $T_2 = 0$. The background noise signal is set to Gaussian white noise. The sampling rate of the system signal is set to 10 kHz and the number of samples is 1 M. The original vibration signals phi1 and phi2 (different initial phase) are shown in Fig. 2.

The original vibration signal is separated by VMD into 2-5 IMFs. Based on the minimum average permutation entropy (0.286), the optimal IMF number of VMD algorithm is set to 2, and the subsequent decomposition results are shown in Fig. 3 and Fig. 4.

As illustrated in Fig. 3 and Fig. 4, the center frequencies of the Intrinsic Mode Functions (IMFs) derived from the Variational Mode Decomposition (VMD) algorithm are situated at 10.0 Hz and 10.1 Hz, exhibiting an initial phase difference of $\pi/2$. Furthermore, the phase difference between IMF1 and IMF2 in the phase signal phi1, and between IMF1 and IMF2 in the phase signal phi2, is also $\pi/2$, which is in good agreement with our simulations. The time difference is determined through cross-correlation between the two vibration signals, which is equal to 0.05 s

Optics EXPRESS

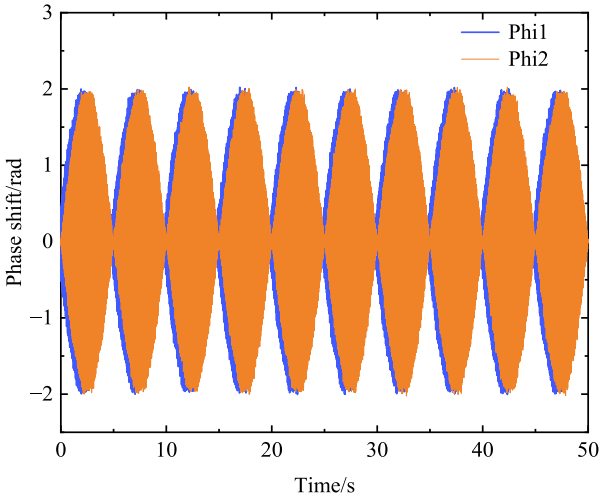

Fig. 2. Near-identical frequency vibration signals in the time domain.

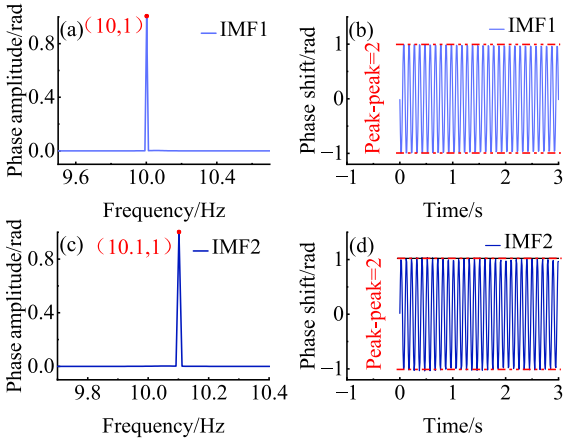

Fig. 3. The IMFs of phi1 decomposed by VMD: (a) 10.0 Hz frequency-domain spectrum; (b) 10.0 Hz time-domain waveform; (c) 10.1 Hz frequency-domain spectrum; (d) 10.1 Hz time-domain waveform.

at 10.0 Hz, and 0.049 s at 10.1 Hz. These results are consistent with the predetermined time differences, thereby demonstrating that the VMD algorithm is capable of effectively decomposing the fundamental characteristics of signals with approximately identical frequencies.

To consider real-world environment conditions, additional simulations were conducted to investigate the algorithm's capability in processing broadband signals. The broadband vibration signals are denoted by phi_i = $a_i + b_i$, a_i = exp(-(t - ti).^2 / (2 * sigma^2)) .* cos(2*pi* f_1*(t - ti)), b_i = exp(-(t - Ti).^2 / (2 * sigma^2)) .* cos(2*pi* f_2*(t - Ti)), where f_1 = 5 kHz, f_2 = 15 kHz, sigma = 0.001, mu1 = 50 ms, t_1 = 0 ms, t_2 = 50 ms, T_1 = 10 ms, T_2 = 50 ms. The sampling rate of the signal is set to 100 kHz and the number of samples per measurement is 20,000. The time-domain and frequency-domain representations of the vibration-induced phase signals phi1 and phi2 are shown in Fig. 5.

Correspondingly, taking the phi1 signal as an example, the VMD yielded results shown in Fig. 5(c)–5(f). The decomposition successfully isolated two broadband signals dominated

Optics EXPRESS

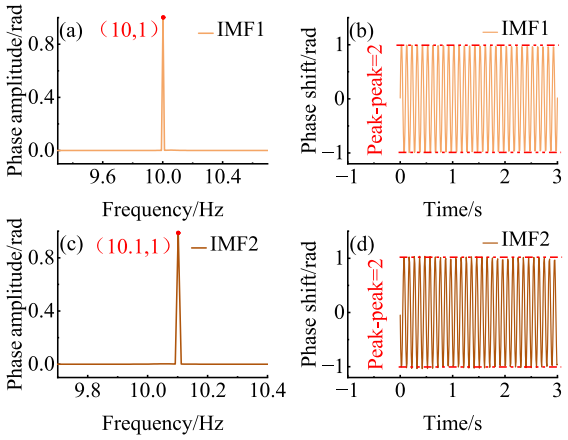

Fig. 4. The IMFs of phi2 decomposed by VMD: (a) 10.0 Hz frequency domain; (b) 10.0 Hz time-domain; (c) 10.1 Hz frequency domain; (d) 10.1 Hz time-domain.

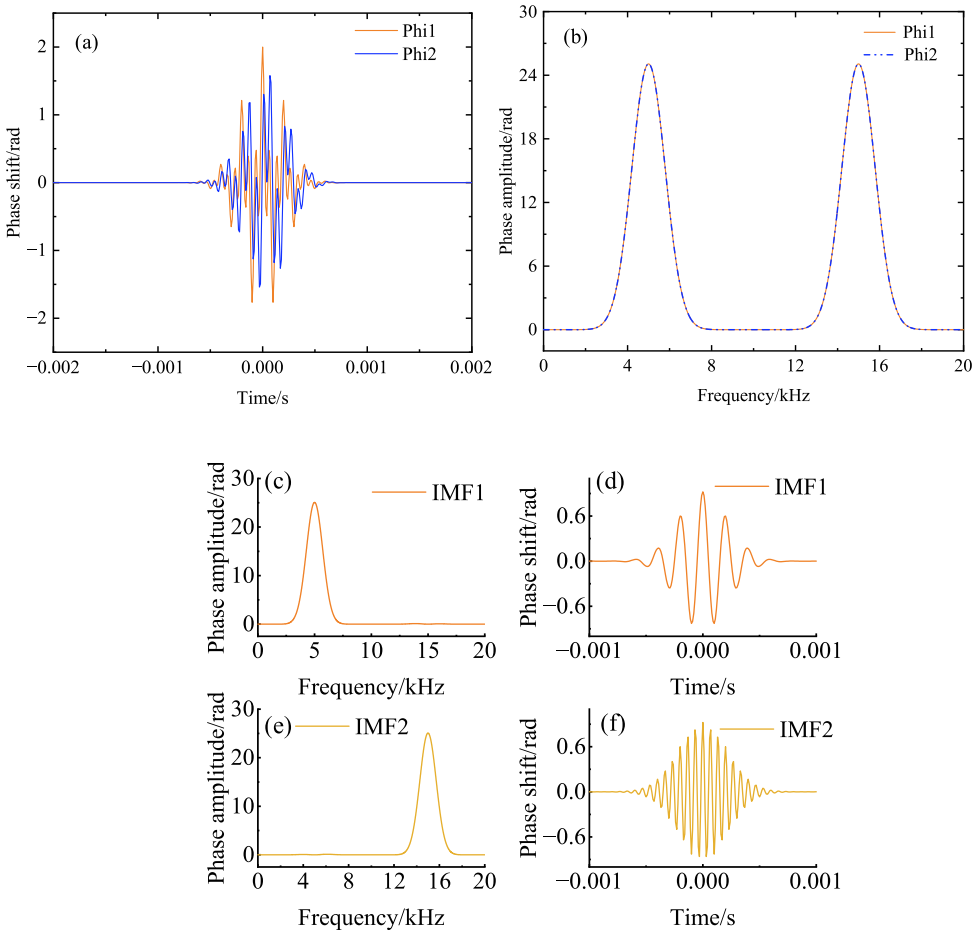

Fig. 5. Broadband vibration analysis: (a) Broadband vibration signals in the time domain, (b) broadband vibration signals in the frequency domain, (c) 5 kHz frequency domain, (d) 5 kHz time-domain, (e) 15 kHz Hz frequency domain, (f) 15 kHz Hz time-domain.

Optics EXPRESS

by frequency bands centered at 5 kHz and 15 kHz. Subsequent cross-correlation analysis between these decomposed IMFs and phi2's IMFs revealed temporal delays of 50 ms and 40 ms, respectively, which align precisely with the preconfigured simulation time delays.

In addition, the spectral superimposition scenario was simulated by configuring two broadband signals at 5 kHz and 7 kHz respectively, with their frequency representations visualized in Fig. 6. Taking phi1 as an example, the decomposition results demonstrate successful separation of the overlapping dominant frequency components. The calculated temporal delays exhibited precise consistency with the preconfigured simulation parameters (50 ms and 40 ms respectively), thereby validating the proposed algorithm's dual capability in processing both broadband signals and near co-frequency signals.

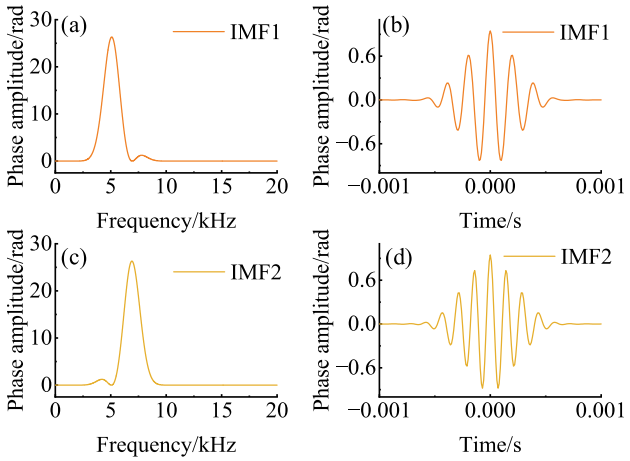

Fig. 6. The IMFs of phi1 decomposed by VMD: (a) 5 kHz frequency domain; (b) 5 kHz time-domain; (c) 7 kHz Hz frequency domain; (d) 7 kHz Hz time-domain.

3. Experimental results and discussion

The Given that this study focuses on investigating the identification and localization of vibration events under extreme scenarios characterized by frequency similarity, the experimental section will primarily involve the analysis of near co-frequency frequency signals. In order to verify the reliability and effectiveness of the VMD algorithm for identification and positioning approximate co-frequency vibration events, both single-point vibration event and multi-point vibration events, of 0.1 Hz and 0.01 Hz frequency differences were demonstrated. The sensing fiber length is 60 km in total, formed by connecting three 20 km fiber spools via FC/APC connectors. The system consists of a highly stable narrow-linewidth laser (NKT E15, 100 Hz linewidth) with a central wavelength of 1550 nm, 4 BDs (400 MHz detection bandwidth), and a 4-channel oscilloscope (50 kSa/s sampling rate, 3 GHz bandwidth). The vibrations were induced by calibrated piezoelectric transducers (PZT) with a frequency response range of 0–25 kHz. To begin with, a single-point vibration was generated at a 10 Hz, located at a distance of 20 km along the sensing fiber, with the result shown in Fig. 7.

Figure 7 illustrates the pre-VMD experiment results obtained at detection end 1. As depicted in Fig. 7(b), the time-domain trace of the vibration signal exhibits a monotonic upward trend. This is predominantly attributed to phase noise and inherent system noise concentrated near the DC component. Furthermore, polarization state may introduce perturbations to the measurement outcomes, which can be mitigated through strategies employing polarization-maintaining fiber and polarization controller. Figure 7(a) shows the vibration signal predominantly comprises

Optics EXPRESS

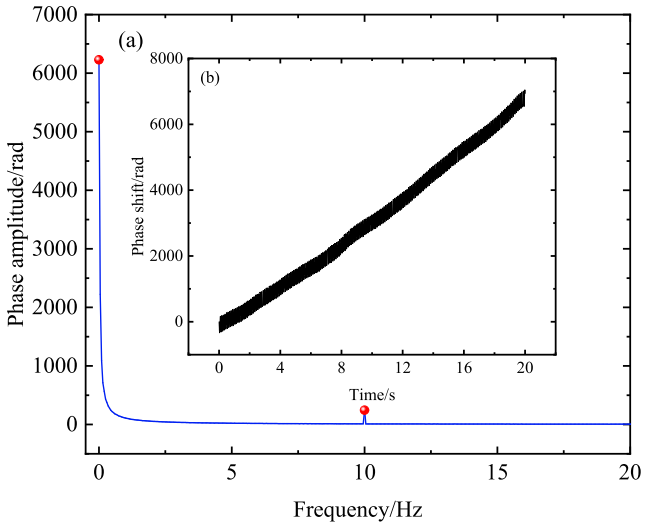

Fig. 7. Single-point vibration response (10 Hz): (a) Frequency-domain phase amplitude spectrum; (b) Time-domain phase shift waveform.

two frequency components (0 Hz and 10 Hz), which suggests that the signal is fundamentally made up of two IMFs. Furthermore, the application of the permutation entropy method reveals that when the number of IMFs is limited to two, the corresponding average permutation entropy is minimized (0.16). After VMD processing is applied, the decomposition results of the two frequencies are shown in Fig. 8, revealing the vibration information resolved as a function of time and frequency.

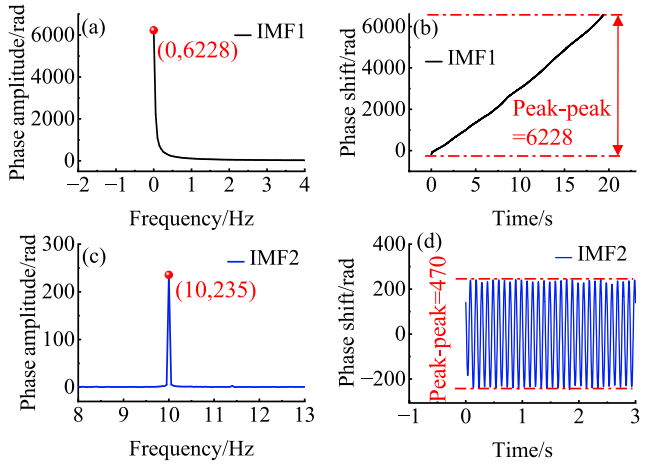

Fig. 8. The IMFs decomposed by VMD (large frequency difference): (a) Frequency-domain spectrum of IMF1; (b) Time-domain waveform of IMF1; (c) Frequency-domain spectrum of IMF2; (d) Time -domain waveform of IMF2.

It can be observed that the main signal characteristics distributed near 0 Hz and 10 Hz have been extracted, indicating that the VMD algorithm can effectively separate the vibration signal (10 Hz) from the raw signal containing noise. Similarly, the IMF with a frequency of 10 Hz at the detection end 2 is obtained using the proposed method, and cross-correlation with IMF2 of

Optics EXPRESS

detection end 1 is performed, with the time-delay results observed at the position is −0.0978 ms. Utilizing Eq. (4) with the effective index (n) of standard telecom single-mode fiber (SMF) set at 1.448 and the speed of light at 299,792,458 m/s, calculations reveal corresponding position for the time delay is 20.22 km. Furthermore, repetitive vibration measurements were conducted to study the repeatability of vibration positioning. A total of 50 consecutive measurements under a 10 Hz disturbance at 20 km were conducted, with the outcomes presented in Fig. 9.

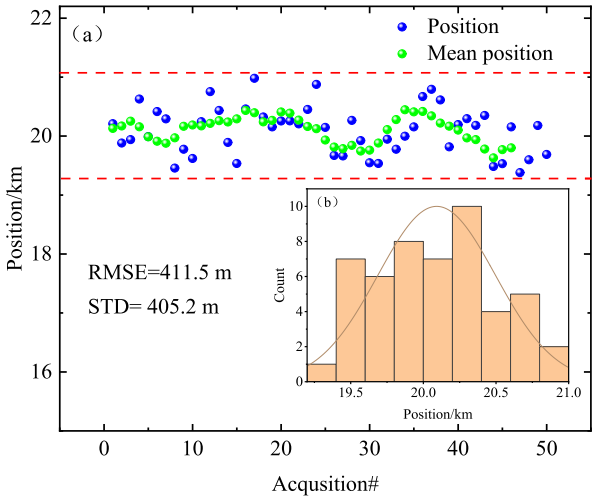

Fig. 9. Vibration position estimation (10 Hz). 5-point moving average was applied for the mean positions, inset: histogram of positions.

The blue circular symbols denote original measurement results, while the green circular symbols indicate the mean value calculated from a moving window of 5 consecutive data points. The experimental results indicate that the actual perturbation position at 20 km (full length being 60 km) is in close agreement with the measured average at 20.092 km, it indicates that the position deviation from the actual value can be reduced to 0.092 km from using zero-mean calibration and a 5-point moving average. As for the positioning accuracy, the system achieved a root-mean-square error (RMSE) of 411.5 m, and a standard deviation (STD) of 405.2 m. It is important to note that the positioning error is significantly worse for lower frequencies (cross-correlation characteristic, usually larger noise amplitudes) and vibrations close to a detection end (larger state-of-polarization mismatch and worse interference visibility).

Figure 10 compares the power spectrum of the vibration signal before and after processing with the VMD algorithm. The results of the experiment indicated that zero-frequency noise was effectively suppressed. Furthermore, the average amplitude of the background noise, processed by the VMD algorithm across a broad frequency spectrum, exhibited a marginal reduction (1.07 dB) when compared to the average amplitude of the background noise prior to the filtering process. Therefore, according to the analysis of experimental results, it can be concluded that the VMD algorithm with tailored coefficients (the number of IMFs and the quadratic penalty factor for limiting the central frequency) can effectively reduce the low-frequency noise and background noise in general, thereby improving the positioning accuracy.

To enhance the analytical capability of the VMD method, four additional sets of vibration events with distinct frequencies (4 Hz, 5 Hz, 6.3 Hz, and 8 Hz) were systematically tested at a 20 km position along the sensing fiber. Figure 11 depicts the positioning results of the 5 vibration events, with the average position at 20.183 km. Additionally, the maximum deviation from the actual position is 0.697 km, which can be significantly reduced by data calibration plus mean-value processing, as demonstrated in the results shown in Fig. 9.

Optics EXPRESS

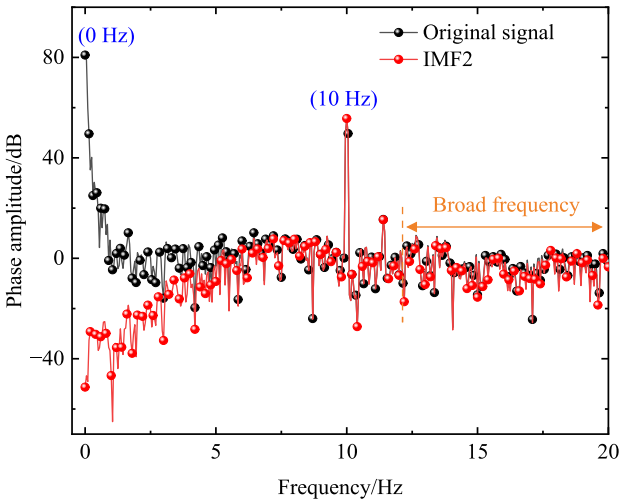

Fig. 10. Power spectrum of the original vibration signal before and after processing with the VMD algorithm. Every 10 data points is plotted as a point.

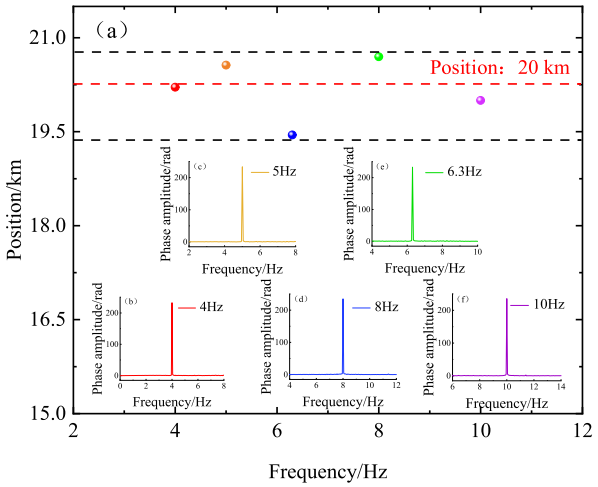

Fig. 11. Single-point vibration position estimation at different frequencies: (a) Vibration position as a function of frequency; Frequency-domain waveform of (b) 4 Hz; (c) 5 Hz; (d) 6.3 Hz; (e) 8 Hz; (f) 10 Hz.

Furthermore, multi-point vibration with approximate co-frequency (10.0 Hz, 10.1 Hz, 10.2 Hz) signals were investigated, where the frequency interval of 0.1 Hz was generated by a signal generator driving PZTs. Specifically, the vibration at 10.1 Hz was identified at a distance of 20 km, while the 10.2 Hz vibration was detected at 40 km, and the 10.0 Hz vibration was observed at 60 km. The experimental results obtained from Detection End 1 are systematically presented in Fig. 12.

As shown in Fig. 12(a), the original vibration signal is primarily composed of four frequency components (0 Hz, 10.0 Hz, 10.1 Hz, 10.2 Hz), and the average permutation entropy reaches its minimum value (0.14) when the number of IMFs is 4. After removing the unwanted noise signal at zero frequency, the decomposition results of the remaining 3 IMFs are shown in Fig. 13.

Optics EXPRESS

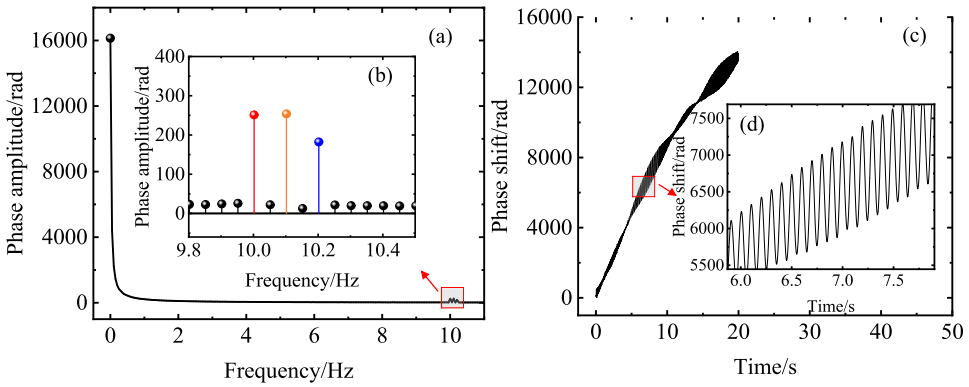

Fig. 12. Multi-point vibration with approximate co-frequency (10 Hz, 10.1 Hz, 10.2 Hz) components: (a) Phase amplitude spectrum, inset (b): details of the frequency-domain; (c) Time-domain phase shift waveform, inset (d): details of the time- domain

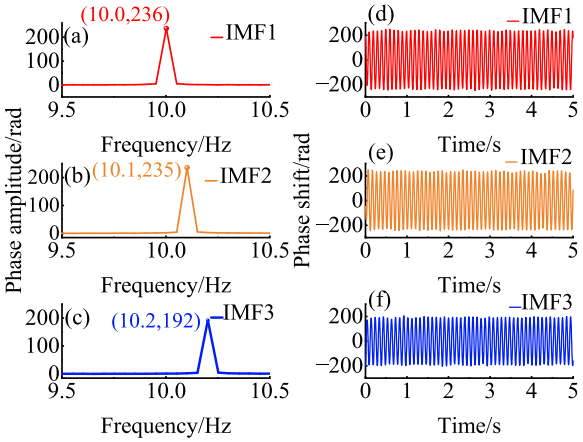

Fig. 13. The IMFs decomposed by VMD (0.1 Hz difference): (a) Frequency-domain spectrum of IMF1; (b) Time-domain waveform of IMF1; (c) Frequency-domain spectrum of IMF2; (d) Time-domain waveform of IMF2; (e) Frequency-domain spectrum of IMF3; (f) Time-domain waveform of IMF3.

From Fig. 13, it can be observed that the frequencies of the three decomposed IMFs correspond precisely to the set frequencies, indicating that the VMD algorithm is effective in decomposing frequency signals with a difference of 0.1 Hz. Using the cross-correlation algorithm, the three vibration events are determined to be located at 20.389 km, 39.223 km, and 59.121 km, respectively.

As an extension, the number of sampling points to 10 M, achieving a frequency resolution of 0.005 Hz (obtained by dividing the sampling rate by the number of sampling points). On this basis, the frequency difference between the three vibration events can be reduced to 0.01 Hz, with the results shown in Fig. 14. The three decomposed IMF components via VMD representing vibration sources are illustrated in Fig. 15. In a similar manner, cross-correlation were conducted on the vibration signals at three distinct frequencies, yielding their respective positions at 19.980 km, 40.020 km and 60.061 km. This finding suggests that enhancement of the frequency resolution of the VMD algorithm can be realized by increasing the sampling rate and the number of sampling points, enabling the acquisition of signals with even closer frequencies.

Optics EXPRESS

However, existing hardware limitations currently cap the maximum number of sampling points that can be processed, e.g. 10 million.

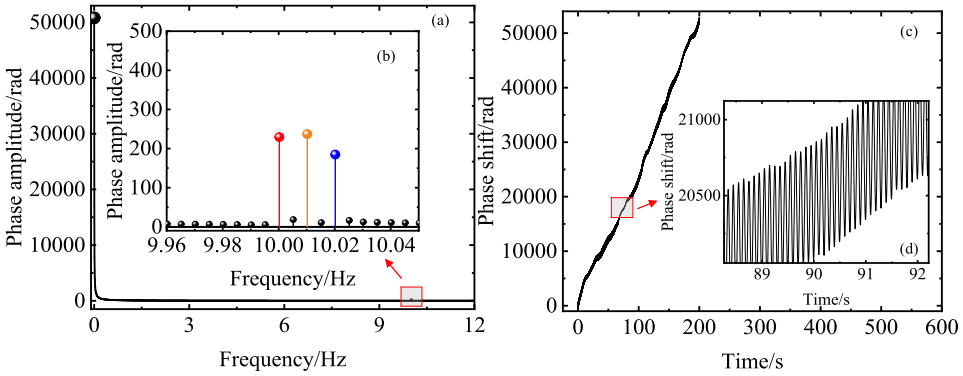

Fig. 14. Multi-point vibration with approximate co-frequency (10 Hz, 10.01 Hz, 10.02 Hz) components: (a) Phase amplitude spectrum, inset (b): details of the frequency-domain; (c) Time-domain phase shift waveform, inset (d): details of the time- domain

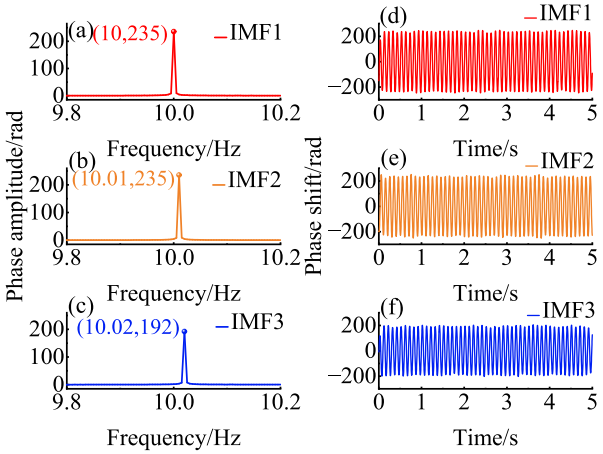

Fig. 15. The IMFs decomposed by VMD (0.01 Hz difference): (a) Frequency-domain spectrum of IMF1; (b) Time-domain waveform of IMF1; (c) Frequency- spectrum waveform of IMF2; (d) Time-domain waveform of IMF2; (e) Frequency-domain spectrum of IMF3; (f) Time-domain waveform of IMF3.

To complete the experimental protocol, the broadband vibration signal positioning was also investigated. The vibration source (PZT) was positioned at the midpoint (20 km) of a 40 km long optical fiber, driven by a function generator delivering broadband excitation signals with spectral dominances at 5 kHz and 15 kHz, as represented in Fig. 16.

The signals acquired from Detection End 1 were decomposed via PE-VMD, with the two intrinsic mode function (IMF) components corresponding to the vibration sources illustrated in Fig. 17. The cross-correlation analysis of these IMFs (Fig. 18) with distinct frequency characteristics yielded vibration positions at 19.638 km (5 kHz component) and 19.980 km (15 kHz component). This experimental result conclusively validates the proposed algorithm's efficacy in processing both broadband signals and even overlapping spectra with near-identical

Optics EXPRESS

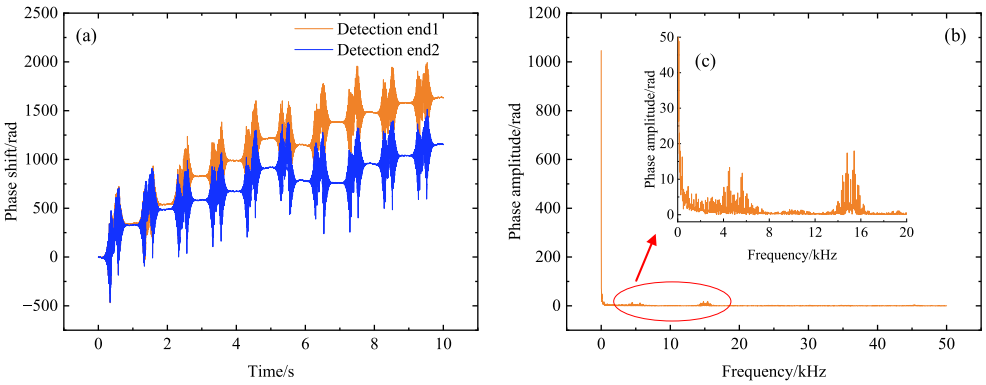

Fig. 16. Multi-point vibration with broadband frequency components: (a) Time-domain phase shift waveform, (b) Phase amplitude spectrum, inset (c): spectral analysis.

central frequencies. In parallel, we present a performance comparison between the proposed algorithm and existing approaches in Table 1.

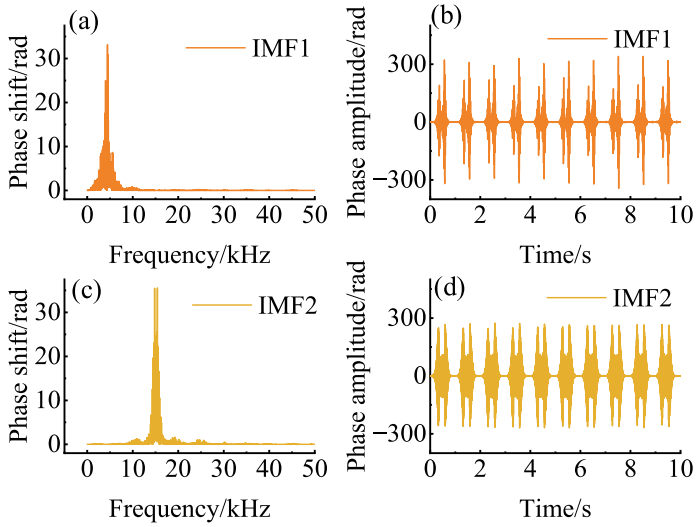

Fig. 17. The IMFs decomposed by VMD: (a) Frequency-domain spectrum of IMF1; (b) Time-domain waveform of IMF1; (c) Frequency- spectrum waveform of IMF2; (d) Time-domain waveform of IMF2.

Table 1. Performance comparison of methods

Method	Frequency Resolution	Single / multi-point vibration positioning	Broadband / single-frequency vibration positioning	Ref.
Cross-correlation	N/A	Single point	Both	[4]
Phase-spectrum time delay	20 Hz	Multi-point	Single frequency	[8]
PE-VMD	0.01 Hz	Multi-point	Both	This work

Optics EXPRESS

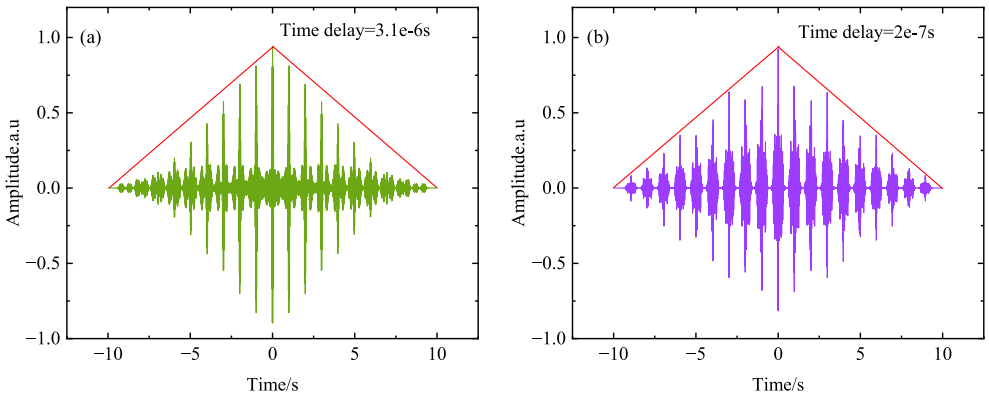

Fig. 18. The time delay estimation based on cross correlation: (a) The IMF1 at the two detection ends, (b) The IMF2 at the two detection ends.

4. Conclusion

Theoretical and experimental studies are carried out on the near-identical frequency signal detection of forward transmission based distributed fiber-optic sensing (FTDS), realized using the adaptation of variational mode decomposition (VMD) and cross-correlation algorithms. Up to three similar-frequency signals with 0.01 Hz separation were analyzed using the proposed method. The single-vibration experimental results (4 Hz to 10 Hz) reveal a positioning accuracy of 411.5 m (RMSE) and 405.2 m (standard deviation) when the vibration frequency is 10 Hz and located at the 20 km position of a 60 km length sensing fiber. The multi-point vibration tests were conducted with vibration events at approximately the same frequency, with frequency differences of 0.1 Hz and 0.01 Hz. The results demonstrated that the sensing system can precisely identify the position of the vibration events. This study indicates that combining the powerful signal extract ability of VMD with long-distance FTDS can realize co-frequency analysis down to 0.01 Hz difference. Additionally, analysis reveals that by increasing the data length (10 M) for signal processing, the proposed method could potentially enable the identification and positioning of multi-point vibration events at even closer frequencies. Furthermore, the proposed method has been successfully validated in multi-point broadband signal vibration positioning along a 40 km sensing fiber, demonstrating its versatility for different applications. This study revealed that the PE-VMD algorithm is versatile, and can operate on broadband/single-frequency vibrations, spectrally adjacent vibrations (0.01 Hz separation), and multiplexed vibration events with precise positioning accuracy, which enables this technology to be utilized for various types of perturbation monitoring.

Funding. National Natural Science Foundation of China (U22A2088, 62275172); Shenzhen Science and Technology Innovation Program (JCYJ20220818095800001, ZDSYS20220606100405013, JCYJ20241202124408012); Scientific Instrument Developing Program of Shenzhen University (2023YQ027); Ling Chuang Research Project of China National Nuclear Corporation; Ministry of Science and Technology of the People's Republic of China (2022YFE0111400).

Disclosures. The authors declare no conflicts of interest.

Data availability. Data underlying the results presented in this paper are not publicly available at this time but may be obtained from the authors upon reasonable request.

References

1. J. Huang, Y. Chen, Q. Song, *et al.*, "Distributed fiber-optic sensor for location based on polarization-stabilized dual-Mach-Zehnder interferometer," Opt. Express **28**(17), 24820–24832 (2020).
2. X. Rao, Y. Wang, M. Chen, *et al.*, "150 km Single-span Distributed Vibration Sensor based on Compensated Self-interference Forward Transmission," J. Lightwave Technol. **42**(16), 5736–5742 (2024).

Optics EXPRESS

3. J. Huang, Y. Chen, H. Peng, *et al.*, "A 150 km distributed fiber-optic disturbance location sensor with no relay based on the dual-Sagnac interferometer employing time delay estimation," Opt. Commun. **479**, 126420 (2021).
4. G. Y. Chen, K. Liu, X. Rao, *et al.*, "Long-range distributed vibration sensing using phase-sensitive forward optical transmission," Opt. Lett. **48**(18), 4825–4828 (2023).
5. S. R. Xie, Q. L. Zou, L. W. Wang, *et al.*, "Positioning error prediction theory for dual Mach-Zehnder interferometric vibration sensor," J. Lightwave Technol. **29**(3), 362–368 (2011).
6. G. Wang, Z. Pang, B. Zhang, *et al.*, "Time shifting deviation method enhanced laser interferometry: ultrahigh precision localizing of traffic vibration using an urban fiber link," Photonics Res. **10**(2), 433–443 (2022).
7. B. Ma, R. Jin, C. Li, *et al.*, "Improved Vibration Localization Algorithm for Multiple Intrusions Based on Phase Spectrum Estimation in Distributed Mach–Zender/Sagnac Optical Fiber Sensing System," IEEE Sensors J. **24**(8), 12426–12432 (2024).
8. X. Rao, S. Dai, M. Chen, *et al.*, "Multi-point vibration positioning method for long-distance forward transmission distributed vibration sensing," Opt. Express **32**(17), 30775–30786 (2024).
9. S. Taoping and L. Zhichao, "Design of pulse and respiration monitoring system based on fiber optic sensing and VMD-FPR processing algorithm," Opt. Fiber Technol. **73**, 103033 (2022).
10. Y. Ma, K. Jia, Y. Song, *et al.*, "Symmetrical Dual In-line Sagnac Fiber Sensor based on VMD-GCC for High Precision Localization," J. Lightwave Technol. **43**(3), 1445–1454 (2025).
11. W. Fu, D. Yi, Z. Huang, *et al.*, "Multiple event recognition scheme using variational mode decomposition-based hybrid feature extraction in fiber optic DAS system," IEEE Sens. J. **23**(22), 27316–27323 (2023).
12. B. Liu, Z. Jiang, and W. Nie, "Negative pressure wave denoising based on VMD and its application in pipeline leak location," J. Mech. Sci. Technol. **35**(11), 5023–5032 (2021).
13. J. Lu, W. Feng, Y. Li, *et al.*, "VMD and self-attention mechanism-based Bi-LSTM model for fault detection of optical fiber composite submarine cables," EURASIP J. Adv. Signal Process. **2023**(1), 29 (2023).
14. H. Wu, B. Zhang, T. Lin, *et al.*, "White noise attenuation of seismic trace by integrating variational mode decomposition with convolutional neural network White noise attenuation using CNN," Geophysics **84**(5), V307–V317 (2019).
15. S. Liu, R. Zhao, K. Yu, *et al.*, "Output-only modal identification based on the variational mode decomposition (VMD) framework," Journal of Sound and Vibration **522**, 116668 (2022).
16. D. Li, *et al.*, "Temperature and acoustic field reconstruction in fiber optic DAS system based on variational mode decomposition," IEEE Sens. J. **24**(10), 16196–16203 (2024).